

ARTICLES

The Spin Mixing Process of a Radical Pair in Low Magnetic Field Observed by Transient Absorption Detected Nanosecond Pulsed Magnetic Field Effect**Tomoaki Miura***Department of Chemistry, Faculty of Science, Shizuoka University, Ohya 836, Shizuoka City 422-8529, Japan***Kiminori Maeda****Physical and Theoretical Chemistry Laboratory, University of Oxford, South Parks Road, Oxford OX13QZ, U.K.***Tatsuo Arai***Graduate School of Pure and Applied Sciences, University of Tsukuba, 1-1-1 tenno-dai, Tsukuba City, Ibaraki Prefecture 305-8571, Japan**Received: November 9, 2005; In Final Form: January 26, 2006*

The spin mixing process of the radical pair in the sodium dodecyl sulfate (SDS) micelle is studied by using a novel technique nanosecond pulsed magnetic field effect on transient absorption. We have developed the equipment for a nanosecond pulsed magnetic field and observed its effect on the radical pair reaction. A decrease of the free radical yield by a reversely directed pulsed magnetic field that cancels static field is observed, and the dependence on its magnitude, which is called *pulsed MARY (magnetic field effect on reaction yield) spectra*, is studied. The observed spectra reflect the spin mixing in 50–200 ns and show clear time evolution. Theoretical simulation of pulsed MARY spectra based on a single site modified Liouville equation indicates that the fast spin dephasing processes induced by the modulation of electron–electron spin interaction by molecular reencounter affect to the coherent spin mixing by a hyperfine interaction in a low magnetic field.

Introduction

The effects of low magnetic fields (<50 mT) on chemical reactions have gotten a lot of attention from the viewpoint of magnetic field effects (MFEs) on biological systems.^{1–3} Especially, the radical pair mechanism is the most considerable mechanism that works in a low magnetic field. Recently, some research groups have proposed the radical pair mechanism as a magnetic compass for the bird navigation from animal's behavior and model calculations of the spin dynamics of the radical pair in low magnetic fields.^{2,3}

In the category of radical pair mechanism, the most important and well-known mechanism that works in low magnetic field is the hyperfine mechanism (HFM),^{1,4–6} which is the change of the efficiency of the coherent electron-spin mixing process between spin sublevels of radical pairs and appears in the comparable magnetic field to the hyperfine interaction (HFI) of them. The MFE by the pure HFM has been observed in the system of electron-transfer reactions in homogeneous solutions, in which the cage lifetime of the radical pair is comparable to that of HFI-induced spin mixing processes (~10 ns).^{1,4–6}

Besides that, the long-lived radical pairs in the artificial linked system^{7,8} and the confined system in super-molecular aggregation^{9,10} are interesting because those are model systems of the

radical pair in a biological environment. In the system of the long-lived radical pairs such as ones generated in micelles, the MFE generated from HFM is distorted by the incoherent longitudinal spin relaxation process (T_1 relaxation).⁹ Because the relaxation time, T_1 , generally depends on the external magnetic field, it is considered as a MFE mechanism, which is called a relaxation mechanism (RM).^{9,11–12} Indeed, the studies on the long-lived radical pair dynamics by MFE have been focused on the RM, which works in a much higher magnetic field than HFI.

In the relatively low magnetic field region, it is important to discuss the relationship between the HFM and the RM from the time domain information of MARY (magnetic field effect on reaction yield) on the basis of the fact that those spin mixing mechanisms have quite different time scales.¹² We have recently developed an analytical method called *time-resolved MARY spectroscopy (TR-MARY)*, which is obtained by plotting the MFE in each observation time window of transient absorption as a function of the applied magnetic field.^{13,14} This method enables us to observe the time evolution of the contribution of RM. Spectra observed at several hundreds of nanoseconds in a micellized radical pair system, however, have shown a higher $B_{1/2}$ value, which is the magnetic field giving half value of saturated MFE, than that expected by pure HFM. The observation of a broad spectrum at 300 ns could not be rationalized by the overlap of HFM and RM¹⁴ because the T_1 value of the

* To whom correspondence should be addressed. E-mail: Kiminori.maeda@chem.ox.ac.uk.

radical pair was estimated to be much longer than 300 ns from Redfield theory.¹⁵ If we observe the MARY spectra in a shorter time scale than hundreds ns, we are able to discuss the origin of the broadening more clearly. The TR-MARY technique, however, has a limitation of the time resolution because it is determined by the rate of the recombination kinetics of the singlet radical pair (k_{rec}).¹³

In the present paper, we propose a novel technique, *pulsed MARY*, which improves the limitation of the time resolution caused by the slow recombination kinetics and enables us to observe the spin mixing process in a short time scale. Our method of nanosecond pulsed MFE is technically based on the fast magnetic field switching on the chemically induced nuclear polarization (SEMF-CIDNP) by Bagryanskaya et al.¹⁶ and on the dynamics of the paramagnetic molecular solid states by Lin et al.¹⁷ However, quantitative and time-resolved measurements of the effect of a pulsed magnetic field on the yield of radical species by transient absorption (TA) have never reported even though they are informative because we can compare the data with the conventional data of TA measurements under a static magnetic field.^{1,9,14} The concept of the present pulsed field technique is similar to that of pulsed reaction yield detected magnetic resonance (pulsed-RYDMR).^{18–21} This technique has been applied to the analysis of the kinetics and the dynamics of the radical pair using good time resolution to its advantage. However, the present pulsed MFE is suitable for the discussion of the spin mixing process of the radical pair from MARY spectra because it is applicable in various external magnetic fields.

For the analysis of pulsed MFE, we have adapted a practical and simple calculation method of the radical pair dynamics that is constructed from the newly combined HFM (in semiclassical approximation)²² and RM. In addition to this, we have taken into account the spin dephasing phenomena that are due to the fluctuation of the electron spin interactions.^{20,23} By this, we have discussed the effect of the spin dephasing on the pulsed MARY curve and have succeeded to simulate the observed data. From theoretical simulations we have presented a novel realization of the spin mixing process in the low magnetic field region.

Experimental Section

A laboratory-made setup for nanosecond TA measurements is similar to the system described elsewhere.²⁴ The third harmonics ($\lambda = 355$ nm) of a pulsed Nd:YAG laser (Spectra Physics GCR-3) and a 500 W Xe lamp (Ushio UXL-500SX) are used as an excitation light source and a probe light source, respectively. The beam from Xe lamp is focused on an end of an optical fiber (core diameter = 0.6 mm), and the other end of the fiber is put into a quartz sample tube. An end of another fiber is faced to the end of the fiber in the quartz sample tube with a gap of 4 mm, in which the photoreaction is initiated by the laser excitation, and a transmitted light is guided into a monochromator (JASCO CT-25). The TA signal is detected by a photomultiplier fixed with a monochromator and recorded with a digital oscilloscope (LeCroy LT-344). The sample solution, which is deoxygenated by bubbling Ar gas before and during the measurement, is transferred into the cell by a flow system. The sample cell is set in a cavity of a conventional electromagnet, which provides a static field.

A nanosecond current pulser is constructed by ARTEK INC. on the basis of the system described in the report by Lin et al.¹⁷ The capacitor bank is charged by applying high voltage (~ 750 V) and discharged instantaneously by a high-speed FET (DEI DE475-102N). The pulsed current is sent to a three-times-

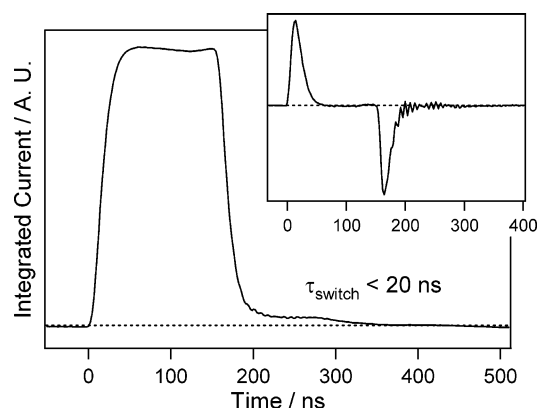


Figure 1. Time profile of nanosecond pulsed magnetic field obtained by numerically integrating the time profile of the induced current in a detection coil, which is shown in the inset.

wound coil whose diameter is 7 mm. Two pulsers are used, and each coil is placed so that the magnetic fields orient in the same direction with a gap of 3 mm and form the Helmholtz coil. The sample cell is placed between two coils. The delay time and duration of pulsed field are controlled by tuning gating pulse signal for FET.

The time profile of a pulsed field is obtained by the induced current detected by a pickup coil settled near the field switching coil. The signal of the pickup coil and its integration are shown in Figure 1. The rise and decay time, both shorter than 20 ns, and the pulse have a flat feature between two edges. We have measured the strength of pulsed field that the sample senses using a MFE on a radical pair reaction, which is estimated at up to 30 mT.

The sample used in this study is sodium dodecyl sulfate (SDS) micellar solution of 2-methyl-1,4-naphthoquinone (MNQ). SDS and MNQ are purchased from Wako Co. Ltd. and used without further purification. Distilled water (Kishida) is used as solvent. The concentration of MNQ and SDS are 1 and 80 mM, respectively.

Theory

The method of calculation in the present work is based on the single site modified Liouville equation model reported previously.^{1,13,14,25}

$$\frac{d|\rho(t)\rangle}{dt} = -(iH^{\times} + \hat{W} + \hat{R})|\rho(t)\rangle \quad (1)$$

In the Liouville equation, the term iH^{\times} represents the spin mixing process by the Zeeman interaction and HFI. One of the most common problems on the practical calculation of the spin dynamics in a low field is the multiplication of the size of electron and nuclear spin space as an increase of the number of nuclear spins in the system. In the calculation, we have used a semiclassical approximation^{22,25} and have set it to the Liouville equation. In the semiclassical model, the HFI is treated as the interaction between the electron spin and the local magnetic field $\mathbf{I}_{a,b}$ that is generated from a vectorial sum of randomly oriented nuclear spins.

$\mathbf{I}_{a,b}$ was assumed to be randomly oriented but to be restricted by the distribution function in the length $I_{a,b}$

$$f(I_i) = (\gamma_i^2/4\pi)^{3/2} \exp\left(-\frac{1}{4}I_i^2\gamma_i^2\right) \quad (2)$$

$$\gamma_i^{-2} = \frac{1}{6} \sum_j a_{ij}^2 J_{ij} (J_{ij} + 1) \quad (3)$$

where a_{ij} and I_{ij} represent the hyperfine coupling constant and nuclear spin quantum number of the j th nuclear interacting with the i th electron spin, respectively.

Thanks to the semiclassical approximation, the spin Hamiltonian is reduced to the operator defined in the space of four basis vectors for two electron spins in Hilbert space as follows.

$$\hat{H} = \sum_{i=1,2} \left(\frac{g_i \mu_B B_0}{\hbar} \hat{S}_{iz} + \mathbf{I}_i \cdot \hat{\mathbf{S}}_i \right) \quad (4)$$

where g_i is the g factor of the i th electron.

\hat{W} and \hat{R} are super operators in Liouville space that represent chemical reactions and spin relaxation, respectively. The rate constants of the escape and recombination reactions are $k_{\text{esc}} = 5.8 \times 10^5 \text{ s}^{-1}$ and $k_{\text{rec}} = 1.5 \times 10^7 \text{ s}^{-1}$, respectively, taken from the previous report.¹⁸

In our calculation, the anisotropic HFI induced relaxation time (T_1 and T_2) is evaluated by Redfield theory with high field approximation as

$$\frac{1}{T_1} = \frac{\tau_c}{6} \frac{[A:A]}{1 + \omega_e^2 \tau_c^2}$$

and

$$\frac{1}{T_2} = \frac{1}{2T_1} + \frac{\tau_c [A:A]}{12} \quad (5)$$

where τ_c , $[A:A]$, and ω_e are the rotational correlation time, anisotropy of HFI, and electron Zeeman frequency of the radical, respectively.¹⁵ The relaxation time of each radical is considered to be equal for simplicity. To be exact, we have a question about the applicability of the high field approximation for MARY in low field. Recently, Fedin et al.²⁶ has calculated anisotropic HFI induced relaxation between eigenstates of radical containing a single nucleus in the low field on the basis of the Redfield theory. According to their report, the rate of population relaxation in the low field is calculated to be much slower than that in the high field, contrary to eq 5, and this theory has been tested by experimental data of time-resolved low field EPR.²⁷ However, the results of their simulation of MARY spectra calculated in that theory differs little from that with high field approximation, suggesting the high field approximation causes little problem in the calculation of MARY spectra.²⁶

Electron–electron spin interactions such as exchange interaction (J) and dipole–dipole interaction (D) strongly depend on inter-radical distance. Therefore, they are fluctuated by the re-encounter process of radical pairs in a comparable time scale to the coherent spin motion. Because of the strong and impulsive but relatively slow fluctuation of the interactions, we can hardly apply the conventional Redfield relaxation theory to such systems. The stochastic Liouville equation (SLE)^{28,29} or Monte Carlo calculation³⁰ is a way for the simulation of fluctuating interactions. However, those calculations take enormous time and need a number of unknown parameters and modeling related to molecular diffusion³¹ and electron–electron spin interactions.

Instead of solving SLE, we have used the effective spin dephasing terms of singlet–triplet dephasing (STD)²³ and triplet–triplet dephasing (TTD)²⁰ phenomenologically. Because the effects of STD and TTD on the spectra are very similar, we cannot determine the parameters for STD and TTD independently. In our calculation, the rate constants of STD and TTD are assumed to be equal ($k_{\text{dephasing}}$). Thus, the super operator for STD and TTD is represented as

$$R_{\text{dephasing}} = k_{\text{dephasing}} \times \left\{ \sum_{i=-1,0,+1} (|ST_i\rangle\langle ST_i| + |T_iS\rangle\langle T_iS|) + \sum_{j=+1,-1} (|T_jT_0\rangle\langle T_jT_0| + |T_0T_j\rangle\langle T_0T_j|) \right\} \quad (6)$$

We solved the Liouville eq 1 and averaged for the nuclear orientations as given by

$$\langle \rho(t) \rangle_{AV} = \int \int \int \int \int \rho(t) f(I_a) f(I_b) \sin \theta_a I_a^2 I_b^2 \sin \theta_b d\theta_a d\theta_b d\varphi_a d\varphi_b dI_a dI_b \quad (7)$$

The integrations for the orientation and the distribution of the nuclear spins are evaluated by the Monte Carlo method. The TA signal is proportional to the sum of the population of the radical pair and escaped free radical, which can be obtained by the time evolution of the density matrix as

$$\Delta A(t) \propto \text{tr} \rho(t) + \int_0^t (k_{\text{esc}} \text{tr} \rho(\tau)) d\tau \quad (8)$$

A time profile of the radical pair is calculated with a single set of randomly sampled nuclear spin configuration, and the calculation of the spectra has converged by averaging 100 times samplings.

Results and Discussion

The photochemical reaction scheme has been reported by Sakaguchi et al.^{9,18} The photoexcited triplet state of MNQ rapidly abstracts the hydrogen atom from the alkyl chain of the SDS micelle to generate a radical pair consisting of a naphthoquinone radical (MNQH \cdot) and SDS alkyl radical (R \cdot) immediately after the laser flash (<30 ns). The TA signal (ΔA_{off}) of MNQH \cdot observed at $\lambda = 380 \text{ nm}$ in the static magnetic field of 25 mT is shown in Figure 2. The decrease of the radical pair and the free radical was observed by the cancellation of the magnetic field with applying a reversely directed pulsed field whose duration and amplitude are 100 ns and 25 mT, respectively, applied at 100 ns after the laser flash.

The schematic explanation of the radical pair dynamics in the pulsed MFE is shown in Figure 3. The radical pair is generated by pulsed laser in the static magnetic field of 25 mT. In the case of triplet born radical pair, the initial population of each triplet sublevel is one-third. In the magnetic field, the efficiency of $T_{+1}-S$ and $T_{-1}-S$ spin mixing due to HFI is much less than that of T_0-S mixing. Therefore, before magnetic field pulse, the population of $S-T_0$ mixed states decays in accordance with the geminate recombination reaction of singlet radical pair, and the T_{+1} and T_{-1} states are over populated. The short pulsed field (pulse width: t_p , field strength: $\Delta B < 25 \text{ mT}$) is irradiated 100 ns after the laser pulse. The magnetic field is reduced to the value B_{mix} by the canceling pulsed field ΔB .

$$B_{\text{mix}} = 25 \text{ mT} - \Delta B \quad (9)$$

Under the transient magnetic field B_{mix} , the $T_{\pm 1}-S$ spin mixing takes place. The spin mixing in the short period results in the population transfer from T_{+1} and T_{-1} states into the $S-T_0$ mixed states. When the magnetic field changes back to 25 mT again after the pulse duration, the T_{+1} and T_{-1} states isolate from the $S-T_0$ mixed states, leaving the transferred population at the $S-T_0$ mixed states. The left populations effectively recombine because of the singlet character of them. Therefore, one can observe the decrease of the radical pair and free radical yield by applying the pulsed magnetic field, as shown in Figure 2.

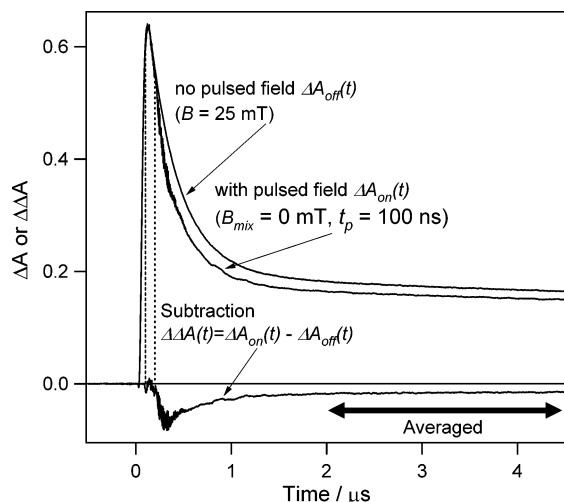


Figure 2. Effect of reversely directed nanosecond pulsed magnetic field to the static field of 25 mT on a time profile of transient absorption. Strength, duration, and delay time of the pulsed field are 25 mT, 100 ns, and 100 ns, respectively. Dashed lines show the time range of pulsed field irradiation.

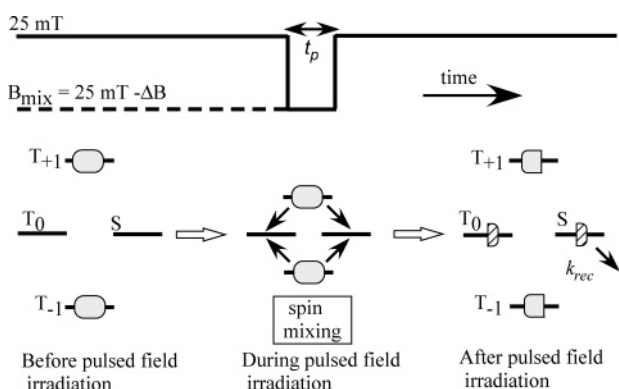


Figure 3. Schematic concept for pulsed magnetic field effect on radical pair dynamics.

The time profile obtained by subtracting the time profile without pulsed field from that with pulsed field shows the rapid rise and slow decay (Figure 2). The time profile of the response to the pulsed magnetic field can be interpreted by the same manner with that for the pulsed RYDMR response.^{18,20} According to the previous paper, the response can be explained by

$$\Delta\Delta A(t) = \Delta A_{\text{on}}(t) - \Delta A_{\text{off}}(t) = -\frac{\Delta P}{2} [(1 - X) \exp\{-(k_{\text{rlx}} + k_{\text{esc}})t\} - (1 - Y) \exp\{-(k_{\text{rec}}/2 + k_{\text{esc}} + k_{\text{rlx}})t\} + (X - Y)] \quad (10)$$

where k_{rlx} represents the depopulating rate of T_{+1} and T_{-1} states and

$$X = \frac{k_{\text{esc}}}{k_{\text{esc}} + k_{\text{rlx}}} \quad Y = \frac{k_{\text{esc}}}{k_{\text{rec}}/2 + k_{\text{esc}} + k_{\text{rlx}}} \quad (11)$$

The rapid rise and the slow decay of $\Delta\Delta A(t)$ correspond to the recombination kinetics from $S-T_0$ states and the depopulation of the $T_{\pm 1}$ states due to longitudinal electron spin relaxation (T_1) in 25 mT, respectively. The important feature here is that

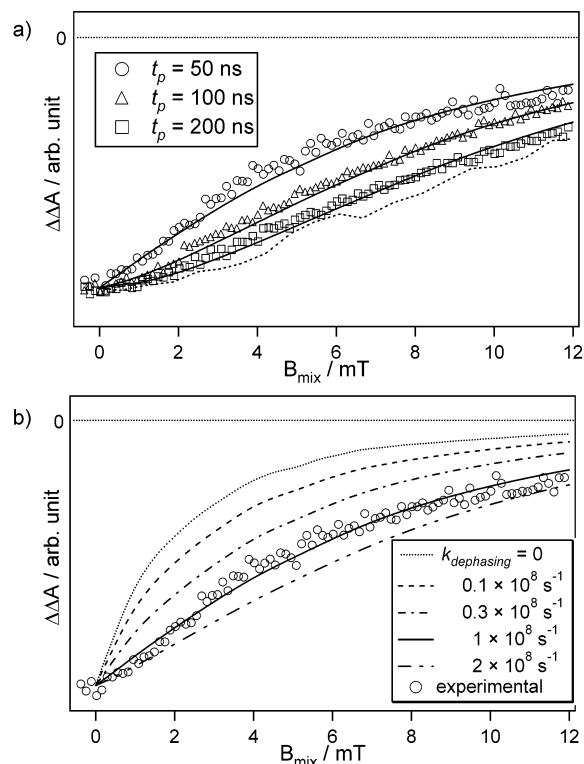


Figure 4. (a) Experimental (O, Δ, and □) and theoretical (—) results of pulsed MARY spectra. Dashed line shows the time-resolved MARY spectra for $t = 300$ ns obtained by static magnetic fields (from ref 14), whose value in $B = 0$ and 25 mT are shifted to normalizing point for pulsed MARY spectra and $\Delta\Delta A = 0$, respectively.¹⁷ (b) Dependence of calculated pulsed MARY spectra in the case of $t_p = 50$ ns on dephasing rate constant shown with observed spectra (O).

the $\Delta\Delta A(t)$ is proportional to ΔP , which is the population transfer from T_{+1} and T_{-1} states to $S-T_0$ mixed states during the period of pulse irradiation. The flat component of $\Delta\Delta A(t)$, which corresponds to the change of free radical yield escaped from micellar cage, is also proportional to ΔP . In later discussion, pulsed field effects are evaluated by the average of $\Delta\Delta A(t)$ in the time region from 2 μs to 4.5 μs , and we call it $\Delta\Delta A$.

Because $\Delta\Delta A$, which is proportional to ΔP , reflects the spin mixing process within a quite short time period of nanosecond pulsed field irradiation, we are able to obtain the field dependence of spin mixing process by observing the dependence of $\Delta\Delta A$ on B_{mix} .

The dependence of $\Delta\Delta A$ on B_{mix} is observed by changing ΔB , which is accomplished by manipulation of the voltage to the current pulsers and is shown in Figure 4a. This field dependence is called *pulsed MARY spectra*. The delay time of the pulsed field irradiation is 100 ns for all experiments. We have observed them with different pulse width and have normalized them to the $\Delta\Delta A$ at $B_{\text{mix}} = 0$ mT, whose scales are 1:1.3:1.7 for three different pulse widths, 50, 100, and 200 ns, respectively. The conventional TR-MARY spectrum observed at 300 ns after the laser pulse, which is the shortest limit at which we could observe it, under the static magnetic field is also presented from ref 14 in Figure 4a (broken line). The pulsed MARY spectrum at $t_p = 50$ ns shows an obviously sharp rise that has never been observed by the conventional TR-MARY spectrum.

The spectral change from $t_p = 50$ ns to 200 ns is very interesting because this time evolution indicates the existence of some factor that modulates the spin mixing dynamics. The earliest stage of the coherent spin mixing by HFI should be

modulated in the time scale under 300 ns. Such quick time evolution of the MARY spectra cannot be explained by the RM under the basis of Redfield theory.

The nanosecond pulsed magnetic field effect on radical pair dynamics is simulated by the manner described above. In the calculation, we have taken the time profile of pulsed magnetic field into account by using time dependent $B_0(t)$ in the spin Hamiltonian. Parameters for the spin relaxation induced by anisotropic HFI are $[A:A] = 5.5 \text{ mT}^2$ and $\tau_c = 33 \text{ ps}$, which are determined by the fitting of TR-MARY spectra with the same model calculation as that present in wider magnetic field region from 0 mT to 250 mT in which the contribution of RM is prominent.¹⁴

The simulated pulsed MARY spectra are shown by solid lines in Figure 4a. The simulation spectra reproduce the time evolution of the MARY spectra and the relative intensity as well. The spectral shape strongly depends on $k_{\text{dephasing}}$, and fast dephasing induces the broadening of it, as shown in Figure 4b. Dephasing time is optimized to 10 ns ($k_{\text{dephasing}} = 1 \times 10^8 \text{ s}^{-1}$), which is similar to that obtained by the nutation experiment of RYDMR carried out by Tadjikov et al.¹⁹ When we use the parameter $[A:A] = 0 \text{ mT}^2$, the calculated pulsed MARY spectra are not changed from those in Figure 4a. This indicates that the dynamic broadening is not caused by anisotropic HFI induced longitudinal relaxation mechanism (conventional RM) but due to the fast dephasing mechanism. The population relaxation time is so long that it does not affect the spin mixing process in such a short time scale (<several hundreds of nanoseconds), whether we adopt the approach by Fedin et al. or not.^{26,27}

The effect of fast dephasing on the coherent $S-T_{\pm 1}$ spin mixing can be explained qualitatively by quantum mechanical calculations of simple two states extracted from spin sublevels of a radical pair. This concept is not quite correct in the proper sense because the spin mixings interfere with each other in multinuclear systems. However, the simple calculation is useful to catch the picture of the spin mixing process graphically. Here, we consider $S-T_{+1}$ spin mixing of the radical pair that has only one magnetic nucleus. The energy gap and the matrix element of the two states are given by

$$\Delta\omega = \langle T_{+1}\beta_N | H | T_{+1}\beta_N \rangle - \langle S\alpha_N | H | S\alpha_N \rangle = \frac{(g_1 + g_2)\mu_B}{2\hbar} B_0 - \frac{a}{4} \quad (12)$$

$$\langle S\alpha_N | H | T_{+1}\beta_N \rangle = \langle T_{+1}\beta_N | H | S\alpha_N \rangle = \frac{-a}{2\sqrt{2}} \quad (13)$$

respectively. In the case of no dephasing, time evolution of the population difference, $P(t)$, between T_{+1} and S states is calculated as follows

$$P(t) = \langle T_{+1}\beta_N | \rho(t) | T_{+1}\beta_N \rangle - \langle S\alpha_N | \rho(t) | S\alpha_N \rangle = \cos \omega' t + \frac{\Delta\omega^2}{\omega'^2} (1 - \cos \omega' t) \quad (14)$$

where

$$\omega' = \sqrt{\frac{a^2}{2} + \Delta\omega^2} \quad (15)$$

and $P(0) = 1$ was used as the initial condition.

When $\Delta\omega = 0$, the two states mix completely and the time average of $P(t)$ is 0, as shown in Figure 5a. If there is a

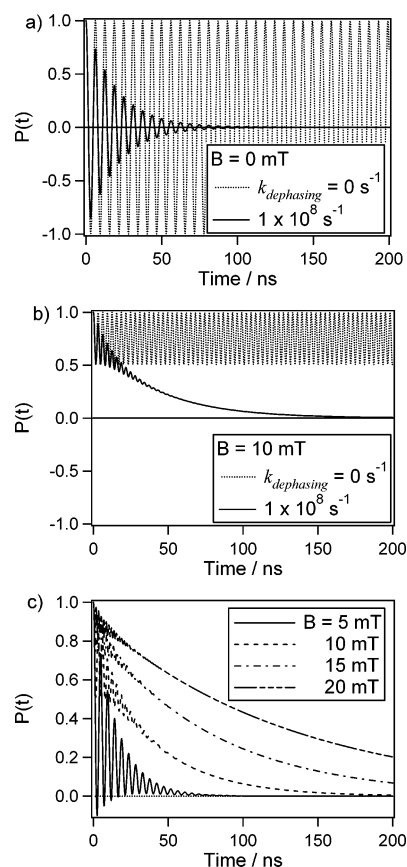


Figure 5. Time evolution of $T_{+1}\beta-S\alpha$ spin mixing of 1 nuclear radical pair calculated by simple two states model. Effective HFI and averaged g value are identical to those in MNQ-SDS system. (a) Spin mixing at $(\hbar\Delta\omega/g\mu_B) = 0 \text{ mT}$ in the presence (—) and absence (·····) of the fast $S\alpha-T_{+1}\beta$ dephasing process. (b) Spin mixing at 10 mT with and without the fast dephasing process. (c) Dependence of the spin mixing on the magnetic field calculated with the fast dephasing process ($k_{\text{dephasing}} = 1 \times 10^8 \text{ s}^{-1}$).

dephasing (STD) between S and T_{+1} spin states, the coherence damps in the time scale of $k_{\text{dephasing}}$ (solid line Figure 5a). However, this process does not change the averaged value of $P(t)$, which is 0 in either case. The time evolution of $P(t)$ in the presence of magnetic field, $\Delta\omega \neq 0$, is shown in Figure 5b. Without dephasing, the averaged $P(t)$ is formulated by

$$\overline{P(t)} = \frac{\Delta\omega^2}{\frac{a^2}{2} + \Delta\omega^2} \quad (16)$$

and the degree of $S-T_{+1}$ coherent mixing is reduced by applied magnetic field (dotted line in Figure 5b). This magnetic field dependence of $\overline{P(t)}$ is the origin of the HFM. In contrast to this, the time evolution of $P(t)$ is much different in existence of the fast spin dephasing between the two states. With fast dephasing, the quantum mechanical oscillation is changed to the incoherent kinetic population transfer with time as shown by the solid line in Figure 5b. In the limit of the fast spin dephasing, the time evolution of $P(t)$ becomes incoherent kinetics completely and the effective time constant of decay of $P(t)$ can be derived analytically, as given by³²

$$\frac{1}{T_1^{\text{eff}}} = \frac{1}{2} \cdot \frac{a^2 k_{\text{dephasing}}}{k_{\text{dephasing}}^2 + \Delta\omega^2} \quad (17)$$

As shown in Figure 5b, the dephasing process increases the mixing efficiency even though it takes longer time than the coherent spin mixing. The broadening of the pulsed MARY spectra is due to the promotion of the $S-T_{\pm 1}$ spin mixing by the dephasing.

The magnetic field dependence of $S-T_{+1}$ spin mixing with fast dephasing is shown in Figure 5c. The rate of incoherent population transfer is reduced by increasing magnetic field, as predicted by the analytical formula of $1/T_1^{\text{eff}}$ in eq 17. The magnetic field dependence on the time scale of the spin mixing appears in the time evolution of the pulsed MARY spectra. In addition to the case of $S-T_{\pm 1}$ mixing, $T_0-T_{\pm 1}$ dephasing (TTD) is considered to affect $T_0-T_{\pm 1}$ mixing even though those two types of spin mixings cannot be separately discussed.

According to our results and the results of pulsed RY-DMR,^{19,20} the value 10 ns of the dephasing time, $1/k_{\text{dephasing}}$ is characteristic for radical pair in micelles. The frequent re-encounter of radical pairs in these systems should be responsible for the fast dephasing. The similar effect of spin dephasing has been hardly observed in the short-lived radical pair in homogeneous solution because the lifetime of the radical pair is shorter than the dephasing time. As shown in Figure 5, the coherent spin dynamics by HFM is dominant in the initial 20 ns. Therefore, a longer lifetime than 20 ns is necessary for observation of the effect of dephasing mechanism. However, if the radical pair lifetime becomes longer by some special intermolecular interaction³³ or the faster spin dephasing is induced by the degenerate electron hopping, we can observe the modulation of the MARY and RYDMR spectra by spin dephasing.³⁴ In other word, the precise analysis of MARY spectra is useful for studying the radical pair dynamics and the molecular interaction as the origin of the dynamics.

Summary

From our experimental result we conclude that the spin mixing process of long-lived radical pairs in low magnetic field can be realized by three stages: (1) coherent spin mixing process by HFI (~ 10 ns), (2) the incoherent spin mixing by HFI assisted by fast dephasing process (~ 100 ns), and (3) incoherent longitudinal spin relaxation process (longer than several hundreds of nanoseconds).

The switching of the three mechanisms appears in the time evolution of MARY spectra. The time evolution of the TR-MARY spectra obtained by TA corresponds to the shift from the second to third stage. On the other hand, we have successfully observed the shift from the first to second stage from pulsed MARY spectra.

Acknowledgment. We express our grateful acknowledgment to Prof. P. J. Hore, Dr. C. R. Timmel, and Prof. Hisao Murai for stimulating discussion of this work. This work was supported by Grant-in-Aid for Development of Scientific Research (No.13740320) from the Japan Society for the Promotion of Science and a Grant-in-Aid for Scientific Research on Priority

Areas (417) from the Ministry of Education, Culture, Sports, Science, and Technology (MEXT) of the Japanese Government. K.M. is indebted by Yazaki Memorial Foundation for Science and Technology, the Kao foundation for Arts and Sciences, Casio Science Promotion Foundation, and Saneyoshi Foundation. T.A. is grateful to a financial support by the Asahi Glass Foundation.

References and Notes

- (1) Steiner, U. E.; Ulrich, T. *Chem. Rev.* **1989**, *89*, 51 and its references.
- (2) Ritz, T.; Adem, S.; Schulten, K. *Biophys. J.* **2000**, *78*, 707.
- (3) Ritz, T.; Thalau, P.; Philips, J. B.; Wiltshcko, W. *Nature* **2004**, *429*, 177.
- (4) Hamilton, C. A.; Hewitt, J. P.; McLauchlan, K. A.; Steiner, U. E. *Mol. Phys.* **1988**, *65*, 423.
- (5) Stass, D. V.; Lukzen, N. N.; Tadjikov, B. M.; Molin, Y. N. *Chem. Phys. Lett.* **1995**, *233*, 444.
- (6) Batchelor, S. N.; Kay, C. W.; McLauchlan, K. A.; Shkrob, I. A. *J. Phys. Chem.* **1993**, *97*, 13250.
- (7) Tanimoto, Y.; Takashima, M.; Hasegawa, K.; Itoh, M. *Chem. Phys. Lett.* **1987**, *137*, 330.
- (8) Lukas, A. S.; Bushard, P. J.; Wasielewski, M. R. *J. Am. Chem. Soc.* **2003**, *125*, 3921.
- (9) Sakaguchi, Y.; Hayashi, H. *J. Phys. Chem.* **1984**, *88*, 1437.
- (10) Horiuchi, M.; Maeda, K.; Arai, T. *App. Magn. Reson.* **2003**, *23*, 309.
- (11) Hayashi, H.; Nagakura, S. *Bull. Chem. Soc. Jpn.* **1984**, *57*, 322.
- (12) Okazaki, M.; Tai, Y.; Nunome, K.; Toriyama, K.; Nagakura, S. *Chem. Phys.* **1992**, *161*, 177.
- (13) Suzuki, T.; Miura, T.; Maeda, K.; Arai, T. *J. Phys. Chem. A* **2005**, *109*, 9911.
- (14) Maeda, K.; Miura, T.; Arai, T. *Mol. Phys.* In press.
- (15) Carrington, A.; McLachlan, A. D. *Introduction to Magnetic Resonance with Applications to Chemistry and Chemical Physics*; Harper & Row: U.S.A., 1967.
- (16) Fedin, M. V.; Bagryanskaya, E. G.; Purto, P. A. *J. Chem. Phys.* **1999**, *111*, 5491.
- (17) Sloop, D. J.; Lin, T.; Ackerman, J. J. H. *J. Magn. Reson.* **1999**, *139*, 60.
- (18) Sakaguchi, Y.; Astashkin, A. V.; Tadjikov, B. M. *Chem. Phys. Lett.* **1997**, *280*, 481.
- (19) Tadjikov, B. M.; Astashkin, A. V.; Sakaguchi, Y. *Chem. Phys. Lett.* **1998**, *283*, 179.
- (20) Gorelik, V. R.; Maeda, K.; Yashiro, H.; Murai, H. *J. Phys. Chem.* **2001**, *105*, 8011.
- (21) Kageyama, A.; Yashiro, H.; Murai, H. *Mol. Phys.* **2002**, *100*, 1341.
- (22) Schulten, K.; Wolynes, P. G. *J. Chem. Phys.* **1978**, *68*, 3292.
- (23) Shushin, A. I. *Chem. Phys. Lett.* **1991**, *181*, 274.
- (24) Miura, T.; Maeda, K.; Arai, T. *J. Phys. Chem. B* **2003**, *107*, 6474.
- (25) Molin, M. Y. *Spin Polarization and Magnetic Effects in Radical Reactions*, Studies in Physical and Theoretical Chemistry; Elsevier: Amsterdam, 1984; Vol. 22.
- (26) Fedin, M. V.; Purto, P. A.; Bagryanskaya, E. G. *Chem. Phys. Lett.* **2001**, *339*, 395.
- (27) Bagryanskaya, E.; Fedin, M.; Forbes, M. D. E. *J. Phys. Chem. A* **2005**, *109*, 5064.
- (28) Pedersen, J. B.; Freed, J. H. *J. Chem. Phys.* **1973**, *58*, 2746.
- (29) Tarasov, V. F.; Bagryanskaya, E. G.; Shkrob, I. A.; Avdievich, N. I.; Ghatlia, N. D.; Lukzen, N. N.; Turro, N. J.; Sagdeev, R. Z. *J. Am. Chem. Soc.* **1995**, *117*, 110.
- (30) O'Dea, A. R.; Curtis, A. F.; Green, N. J. B.; Timmel, C. R.; Hore, P. J. *J. Phys. Chem. A* **2005**, *109*, 869.
- (31) Hore, P. J.; Hunter, D. A. *Mol. Phys.* **1992**, *75*, 1401.
- (32) Hore, P. J. Ph.D. Thesis.
- (33) Matsuyama, A.; Murai, H. *J. Phys. Chem. A* **2002**, *106*, 2227.
- (34) Justinek, M.; Grampp, G.; Landgraf, S.; Hore, P. J.; Lukzen, N. N. *J. Am. Chem. Soc.* **2004**, *126*, 5635.